



Computational Issues in Modeling Ion Transport in Biological Channels: Self-Consistent Particle-Based Simulations

S. ABOUD AND M. SARANITI

*Molecular Biophysics Department, Rush University, Chicago, IL, USA; Electrical and Computer
Engineering Department, Illinois Institute of Technology, Chicago, IL, USA*

R. EISENBERG

Molecular Biophysics Department, Rush University, Chicago, IL, USA

Abstract. In this work, a self-consistent Langevin dynamics simulator will be presented, and computational issues unique to the simulation of charge transport through ion channels will be addressed. The simulation approach is divided into two parts; the first is the development of an efficient model to account for the charge transport in bulk electrolyte solutions, while the second is the accurate representation of the channel protein and lipid structure. A cavity is made in the interior of a phospholipid bilayer and an ion channel is inserted, where the atomic coordinates of the protein are obtained from experimental work. The electrostatic potential felt by a potassium ion along the center of the channel is then calculated and comparisons are made between two types of potassium channels, KcsA and MthK.

Keywords: Langevin dynamics, ion channels, lipid bilayer, KcsA, MthK, nonequilibrium ionic transport

1. Introduction

Ion channels are a class of proteins embedded in cell membranes, and form conduction pores that regulate the transport of ions into and out of cells. These pore proteins are present in all living organisms and play a crucial role in many biological functions, including electrical signaling in the nervous system, hormone secretion, and heart and muscle contraction [1]. Not only are ion channels important in their biological purpose, they are also extremely interesting for their possible use in bio-electronics, more specifically as a component in a new class of bio-sensors. Therefore, the development of efficient modeling techniques to accurately describe the permeation of charge carriers through these ion channels is important for a wide range of applications.

Potassium (K^+) channels are a large class of ion channels that share important features of their amino acid sequence. In particular, K^+ channels generally have identical selectivity filters [1], which are crucial

for permeation because they are directly responsible for allowing a specific ion species to flow through the channel pore. In addition, recent experimental works [2,3] have made significant progress toward understanding the key components of K^+ channels at an atomistic level and their role in both selectivity and gating, which is the property of switching between open or closed conductive states as a response to electrical, chemical, or mechanical stimuli.

Brownian dynamics type simulations are widely used for modeling transport in ion channels [4–8]. This is primarily because they can be used to simulate the long time scales (μs) that are relevant in biological systems without requiring unreasonable computer resources. The drawback of these approaches is the loss of microscopic information. In fact, interactions at the atomic level are modeled by macroscopic quantities such as the dielectric constant or the diffusion coefficient, which are often not well suited to describe charge transport at the atomic-scale dimensions required by

many, but not all, ion channels. Indeed, several works have shown that channel conductance is very sensitive to the choice of dielectric constant used for the pore cavity and the protein [9,10].

In this work, we use a Brownian dynamics simulator based on the Langevin equation to solve for the ionic transport, and include an atomistic representation of the ion channel protein and lipid bilayer. The atomic coordinates and charge distribution of the system are obtained using experimental results and the software package GROMACS [11].

In the next section, the self-consistent Brownian dynamics simulator will be presented and bulk electrolyte solution results will be shown. Numerical issues related to the charge transport in this region, including boundary conditions and electrostatic forces are discussed. In the following section the method used to insert the lipid and ion channel structures into the simulation domain will be presented. Results of the electrostatic potential distribution for two types of K^+ channels will be presented and discussed.

2. Brownian Dynamics

The simulation approach used for modeling the ion transport in the bulk electrolyte solution is based on an iterative scheme in which the solution of the Langevin equation [12] is self-consistently coupled with a P^3M algorithm [13,14] used to resolve the spatial distribution of the electrostatics forces. The primitive model is used to account for the water bath in which the ions are suspended. In this way, each ion is treated as a Brownian particle in a continuum dielectric and tracked through the 6-dimensional phase space. Therefore, the ion-solvent interactions are modeled through macroscopic water properties, which include the dielectric constant and friction coefficient [15,16].

The short-range component of the force, including both the Columbic interaction and finite-size effects of the ions is calculated using an inverse power relation [5,13], which depends on both the ionic radius and the strength of the repulsion between ions. The long-range interaction, which includes the external boundary conditions, is calculated through the solution of Poisson's equation, using an iterative multigrid approach [17]. The nearest-grid point method is used for the charge assignment and field interpolation schemes.

The simulation domain used to calibrate the bulk electrolyte solution is a homogenous $20 \times 20 \times 20$

tensor product grid with mesh spacing 0.5 nm in all three directions. In this work, Dirichlet boundary conditions are used to mimic the electrostatic behavior of idealized "electrodes", and are located on opposite planes of the 3D volume, while Neumann conditions are imposed on the other 4 planes. Ions are reflected from the Neumann boundaries, while are allowed to cross freely through the Dirichlet contacts. The simulated volume represents a portion of a larger electrolyte bath, so the total molar concentration in the electrode regions is conserved at each time step though injection and ejection of ions. The velocity of the injected ions is calculated according to a Maxwellian distribution in the directions parallel to the contacts, while a half-Maxwellian injection is used normal to the contacts.

The calculated equivalent conductivity for several aqueous KCl solutions under nonequilibrium conditions is shown in Table 1, and is in very good agreement with experimental values [18], at several molar concentrations. As can be seen, the simulated values of the conductivity tend to deviate at higher molar concentrations. This is due to a break down in the validity of the primitive water model, due to the fact that at high concentrations the average distance between ions becomes comparable to the diameter of the water molecules [19].

As a further test of the approach used for the simulation of bulk ionic solutions, the radial distribution function (or pair correlation function) is calculated, and the results are shown in Fig. 1. The radial distribution function is a measure of the liquid structure and is of central importance because it can be used to obtain a complete description of the thermodynamic state of the system [15]. The computed radial distribution function shows qualitative agreement with continuum water models. In particular, the distribution goes to zero for distances less than the inter-ionic diameter and to one for large separations, which is consistent with analytic approximations [15].

Table 1. Simulation and experimental equivalent conductivity in aqueous KCl solution at 298 K for several molar concentrations.

KCl concentration [M]	Equivalent conductivity [$\text{cm}^2 \Omega^{-1} \text{mol}^{-1}$]	
	Simulation	Experiment [19]
0.1	125.2	128.96
0.2	120.6	123.90
0.5	119.5	117.20
1.0	123.3	105.81

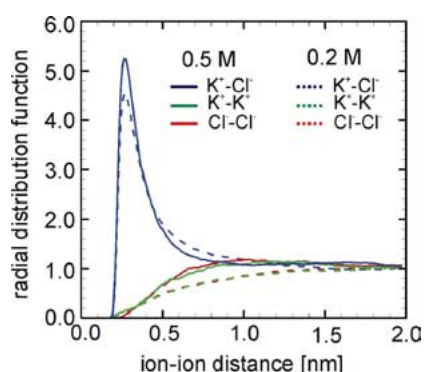


Figure 1. Radial distribution function in aqueous KCl solutions at 298 K, for molar concentrations of 0.5 M and 0.2 M.

3. Ion Channel and Lipid Bilayer

The atomic coordinates and charge distribution of the channel protein and lipid membrane are inserted explicitly in the simulation domain using a combination of experimental data and simulation results. The atomic coordinates of the ion channel are obtained from x-ray diffraction experiments of crystallized proteins [2,3], available in the Brookhaven Protein Database (PDB files) [20]. An energy minimization based approach [21] is then applied to insert the channel into the interior of a phospholipid membrane, which is obtained by molecular dynamics simulations [22] and is also available as a PDB file.

Although a real cell membrane is generally made up of several different types of lipid molecules [23], the channel proteins in these simulations are embedded into a bilayer composed of individual palmitoyl-oleoyl-phosphatidylcholine (POPC) phospholipids. The initial starting structure is a rectangular bilayer patch consisting of 512 POPC lipids, adjoined by 9840 molecules of water [22]. A cavity is created in the interior of the membrane to match the outer surface of the ion channel protein, using an updated MDRUN function that is added to GROMACS [11]. This version of the function reads the external surface of the ion channel protein, and exerts an outward force on any lipid atom that would be located inside. The atoms in the protein are treated as van der Waals spheres [23] and the surface is determined by retaining the portion of the spheres that comprise the external molecular boundary. The software package MSMS [24] is used to calculate the surface, with a probe radius of 1.4 Å. After an appropriate hole has been made in the membrane, the ion channel is inserted into the hole and the en-

tire system is equilibrated using a steepest decent energy minimization procedure supplied by GROMACS [20]. The simulations are run at constant particle number, pressure and temperature. An anisotropic pressure coupling constant of 1.0 ps is used, and the coupling constant for the temperature bath is 0.1 ps. The force constant for the repulsive force on the lipids due to the protein surface is 10 kJ/mol/nm for 20 ps followed by 100 kJ/mol/nm for another 20 ps. The GROMACS87 force field is used with an electrostatic cutoff of 1.8 nm. All other parameters are obtained from [21].

The atomic charge distribution is then calculated from GROMACS and the entire system is inserted into a $70 \times 40 \times 40$ grid with a homogenous mesh of 0.3 nm and a dielectric constant of 78. Currently, the atoms are treated as a static charge distribution and both the long-range and short-range components of the electrostatic interaction are computed.

4. Results

To demonstrate the robustness of this approach, the electrostatics of two K^+ channels is investigated. The KcsA [2] channel is an example of a voltage-gated structure, while MthK [3] is an example of a ligand (in this case calcium) gated channel. The molecular structures of these channels correspond to an *open* configuration for MthK and a *closed* configuration for KcsA.

The molecular representation of two side chains of the atomic coordinates for the MthK K^+ channel embedded in a POPC lipid membrane is shown in Fig. 2. The individual atoms lining the selectivity filter are explicitly illustrated, in order to show the binding sites of the K^+ ions. A positive point-charge is placed at several positions along the channel and the electrostatic force acting on it is calculated. The force is determined by the solution of the Poisson equation combined with the short-range, repulsive Coulomb interaction, no finite volume effects have been included in the calculation. The electrostatic potential profile along the channel is then calculated by integrating this force. The potential profile of the MthK and KcsA channel is shown in Figs. 3 and 4, respectively. The KcsA profile agrees very well with results found in literature [6], while the MthK channel shows different electrostatic features than the KcsA channel. The potential well at the intracellular side (~ 1.0 nm in the graph) of the KcsA is due to a ring of negatively charged amino acids at the end of each inner helix. As the channel opens, the helices

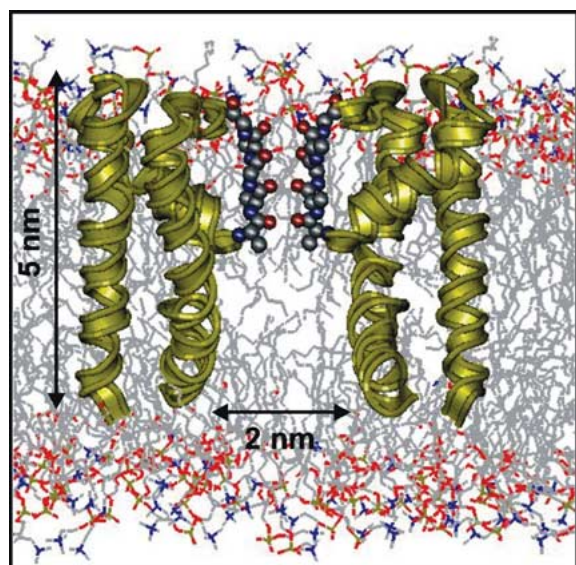


Figure 2. Two side chains of the MthK K^+ channel structure embedded in an explicit POPC lipid bilayer. The atoms lining the selectivity filter are represented as spheres to show the individual “cages” which represent the binding sites of the K^+ ion.

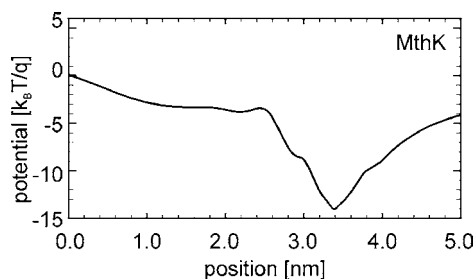


Figure 3. The integral of the total electrostatic force acting on one K^+ ion as a function of position along the center of the MthK channel. The open structure is evident from the lack of any barrier at the opening of the channel.

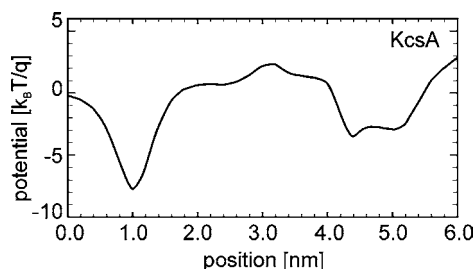


Figure 4. The integral of the total electrostatic force acting on one K^+ ion as a function of position along the center of the KcsA channel. Ions coming from the bulk solution on the left see a potential well that traps them before they can enter the channel.

separate, decreasing the depth of this attractive potential [6,11], as it can be seen in the open MthK channel, due to the larger separation of the side chains. A particularly interesting feature in these plots is the potential profile in the region of the selectivity filter, which has an identical amino acid sequence in both proteins. In that region, both channels exhibit a potential well, which is deeper in the MthK channel. In addition, the features in the potential are more pronounced in the potential energy profile of MthK when the testing point charge is replaced by a K^+ ion with a finite size. The influence of the excluded volume interaction clearly plays a crucial role in the ionic charge transport within the channel and will be further investigated to determine the specific structure of the selectivity filter and its transport properties.

5. Conclusion

The atomic structure of the KcsA and MthK K^+ ion channels have been embedded into a POPC lipid membrane and the entire structure has been included in a self-consistent Langevin dynamics solver. The corresponding electrostatic potential profiles have been shown for *open* and *closed* channel structures. The atomic coordinates of both the protein and lipid bilayer have been treated as static quantities in this work. In reality, the motion of the charge distribution in the protein structure may significantly influence the ionic transport, particularly in the region of the selectivity filter. Further work needs to be done to investigate the influence of the motion of the ion channels components at the atomic scale on the electrostatic characteristics, as well as the correct form of the short-range electrostatic interaction. The impact of water molecules in the channel must also be examined.

Acknowledgments

This work was supported in part by the National Institute of Health T32 HL07692. The authors would like to thank Dr. Larry Scott and Dr. Wolfgang Nonner for their helpful suggestions.

References

1. B. Hille, *Ionic Channels of Excitable Membranes*, Sinauer, Massachusetts (1992).

2. D.A. Doyle, J.M. Cabral, R.A. Pfuetzner, A. Kuo, J.M. Gulbis, S.L. Cohn, B.T. Cahit, and R. MacKinnon, *Science*, **280**, 69 (1998).
3. Y. Jiang, A. Lee, J. Chen, M. Cadene, B.T. Chait, and R. MacKinnon, *Nature*, **417**, 515 (2002).
4. C. Millar, A. Asenov, S. Roy, and J.M. Cooper, *Journal of Computational Electronics*, **1**, 405 (2002).
5. M. Saraniti, S.J. Wigger, Z. Schuss, and R.S. Eisenberg, in *Proceedings of 2002 International Conference on Modeling and Simulation of Microsystems- MSM2002* (S. Juan, PR, April 2002).
6. R.J. Mashl, Y. Tang, J. Schnizer, and E. Jakobsson, *Biophysics Journal*, in press.
7. W. Im and B. Roux, *Journal of Chemical Physics*, **115**, 4850 (2001).
8. S.-H. Chung, T.W. Allen, and S. Kuyucak, *Biophysics Journal*, **82**, 628 (2002).
9. M.B. Partenski and P.C. Jordan, *Journal of Physical Chemistry*, **96**, 3906 (1992).
10. C.N. Schultz and A. Warshel, *Proteins*, **44**, 400 (2001).
11. www.gromacs.org
12. P.E. Kloeden and E. Platen, in *Applications of Mathematics* (Springer-Verlag, 1999).
13. R.W. Hockney and J.W. Eastwood, *Computer Simulation Using Particles* (Adam Hilger, Bristol, 1988).
14. C.J. Worldelman and U. Ravaioli, *IEEE Transaction of Electron Devices*, **47**(2), 410 (2000).
15. D.A. McQuarrie, *Statistical Mechanics* (University Science Books, Sausalito, CA, 2000).
16. V. Bacilon, D. Chen, R.S. Eisenberg, and M.A. Ratner, *Journal of Chemical Physics*, **98**, 1193 (1993).
17. W. Hackbush, *Multi-Grid Methods and Applications* (Springer-Verlag, Berlin, 1985).
18. V.M.M. Lobo, *Electrolyte Solutions: Literature Data on Thermodynamic and Transport Properties*, (Coimbra, 1975) vol. 2.
19. J.M.G. Barthel, *Physical Chemistry of Electrolyte Solutions, Topics in Physical Chemistry 5* (Springer, Steinkopf, 1998).
20. H.M. Berman, J. Westbrook, Z. Feng, G. Gilliland, T.N. Bhat, H. Weissig, I.N. Shindyalov, and P.E. Bourne, *The Protein Data Bank, Nucleic Acid Research*, **28**, 235 (2000).
21. J.D. Faraldo-Gómez, G.R. Smith, and M.S.P. Sansom, *European Biophysics Journal*, **31**, 217 (2002).
22. D.P. Tieleman, M.S.P. Sansom, and H.J.C. Berendsen, *Biophysics Journal*, **76**, 40 (1999).
23. J.M. Berg, J.L. Tymoczko, and L. Stryer, *Biochemistry* (W.H. Freeman and Company, New York, 2002).
24. M.F. Sanner, A.J. Olson, and J.C. Spohner, *Biopolymers*, **38**, 305 (1996).